Journal of Magnetic Resonance **142,** 145–152 (2000)
Article ID jmre.1999.1922, available online at http://www.idealibrary.com on IDEAL®

Multiple-Quantum Cross Polarization in Quadrupolar Spin Systems during Magic-Angle Spinning[1]

David Rovnyak, Marc Baldus, and Robert G. Griffin

MIT/Harvard Center for Magnetic Resonance, Francis Bitter Magnet Laboratory and Department of Chemistry, Massachusetts Institute of Technology, Cambridge, Massachusetts 02139

Received June 3, 1999; revised August 18, 1999

We describe the concept of multiple-quantum cross polarization (CP) between an $I = \frac{3}{2}$ and an $I = \frac{1}{2}$ spin during magic-angle spinning. Experimental and theoretical results for ^{23}Na–^{1}H pairs are presented that elucidate the transfer mechanism and the beneficial effect of adiabatic amplitude modulations of the CP field. The multiple-quantum CP approach is shown to be beneficial for improving the sensitivity of CP-MQMAS experiments and for detecting dipolar correlations. © 2000 Academic Press

Key Words: **solid-state NMR; multiple-quantum MAS (MQMAS); rotation-induced adiabatic coherence transfer (RIACT); dipolar coupling; radiofrequency amplitude modulation.**

INTRODUCTION

During the past few years there has been enormous progress in addressing one of the outstanding problems of solid-state NMR, namely, the observation of high-resolution spectra of half-integer quadrupolar nuclei. Spectroscopy of quadrupolar systems is important since they represent ~70% of the periodic table and are intimately involved in many chemical, physical, and biological processes (*1*). Until recently, these spin species have been largely NMR silent, but the introduction of multiple-quantum magic-angle spinning (MQMAS) has dramatically altered this landscape (*2*). Specifically, by correlating the evolutions of multiple-quantum and central-transition coherences, it is possible to extract isotropic spectra in either a one- or two-dimensional experiment (*3–5*). With this methodology, high-resolution spectra of $S \geq \frac{3}{2}$ species with $\omega_Q \leq 600$ kHz (*3, 6–11*) can be recorded, where $\omega_Q = (e^2qQ/h)/[2S(2S-1)]$.

Despite our ability to observe high-resolution spectra of quadrupolar spins in a number of cases, there remain many problems to address. For example, the multiple-quantum excitation efficiency in all versions of MQMAS is low and significantly limits the applicability of the technique. Further, in many cases the quadrupole T_1 values are long, exacerbating the already acute signal-to-noise problem. In situations like these involving $I = \frac{1}{2}$ systems, it is customary to turn to one of the many variants of cross polarization (*12, 13*) to both enhance signal intensities and shorten the effective spin–lattice relaxation times. For example, for proton-coupled $I = \frac{1}{2}$ systems, the CP transfer alone can lead to enhancements of the magnetization of $\sim\gamma_S/\gamma_I$, where the γ_i are the gyromagnetic ratios of the spins involved.

In $I = S = \frac{1}{2}$ spin systems, the spin dynamics for cross polarization are well understood (*14–17*), but for quadrupolar spin systems, this is not the case. In particular, in either static (*18, 19*) or rotating samples (*20, 21*), the spectroscopy and spin dynamics are dominated by the quadrupole interaction (*22–25*). For this reason, cross-polarization experiments to date have focused on polarizing the central transition by employing a small B_1 for spin locking (*20, 21, 26–30*). In the context of high-resolution multiple-quantum MAS (MQMAS) experiments (*2, 3*), the CP step is followed by excitation (*29*) and reconversion (*30*) of multiple-quantum coherence for observation. Since low RF power is employed in this approach, it is common to observe poor frequency offset performance and low spin-locking efficiencies for the CP process.

In this contribution, we investigate the CP dynamics of an $I = \frac{3}{2}$ nucleus coupled to an $S = \frac{1}{2}$ nucleus during MAS. We show that a triple-quantum CP (TQCP) process during MAS permits the use of high-power spin-locking fields and improves the sensitivity in CP-MQMAS spectra. We also demonstrate the improved polarization transfer characteristics of an amplitude-modulated TQCP transfer and the ability to perform spectral filtering.

THEORY

In spin-$\frac{1}{2}$ applications, a theoretical analysis of the CP dynamics is often performed by considering an isolated $I = \frac{1}{2}$, $S = \frac{1}{2}$ spin pair (*31*). In this case, strong radiofrequency (RF) fields dominate all other interactions in the system Hamiltonian and the spin-lock field can be described in a tilted rotating frame in which the eigenvectors are related to the high-field eigenstates (where k, $l = \pm\frac{1}{2}$ represent the magnetic quantum numbers) by a simple rotation given by $\exp[i(I_y + S_y)(\pi/2)]$. In this frame, the initial conditions I_x, S_x are diagonal, which justifies the concept of *polarization* transfer under strong RF

[1] Presented in part at the 39th ENC Conference, Asilomar, CA, 1998.

1090-7807/00 $35.00

fields. The dynamics and matching conditions in an isolated two-spin system can be derived using average Hamiltonian theory (*32*) (AHT) or Floquet theory (*33–35*).

In contrast to the spin-$\frac{1}{2}$ case, Vega has shown (*20, 21*) that the quadrupolar contribution usually dominates the Hamiltonian of an $S = \frac{3}{2}$ system, even during rapid MAS modulation. To describe the phenomenon of spin locking and CP, we will first investigate the spin-lock behavior of an isolated quadrupolar nucleus S. In addressing this problem, Vega suggested an approach where the influence of the quadrupolar interaction upon the spin lock and CP characteristics can be viewed by a time evolution of the eigenstates (*21*). In contrast, we describe the time dependence of the quadrupolar coupling with an effective RF Hamiltonian, which is useful in the description of homonuclear recoupling (*36*). One can compare both approaches with the usual selection of a Schrödinger or Heisenberg picture (*37*) to describe the explicit time dependence of the system.

We begin by treating an isolated $S = \frac{3}{2}$ spin during MAS. In the rotating frame, the RF and quadrupolar terms in the Hamiltonian are

$$H = \omega_S S_x + H_Q, \qquad [1]$$

where we have neglected isotropic chemical shift terms to simplify the analysis. The quadrupolar contribution to the total spin Hamiltonian is treated with first-order perturbation theory with respect to the Zeeman interaction and is given by

$$H_Q = A_{20}(t)T_{20} + \frac{1}{\omega_0}\sum_{m=\pm1,\pm2}\frac{1}{m}A_{2m}(t)A_{2-m}(t)[T_{2m}, T_{2-m}]. \qquad [2]$$

The time dependence of the spatial components can be described by a series expansion in which the reduced Wigner elements d_{nm} are evaluated at the magic angle θ_m:

$$A_{2m}(t) = \sum_{n=\pm1,\pm2} A_{2n}d_{nm}(\theta_m)\exp[in\omega_r t]. \qquad [3]$$

The spatial tensor components in the rotor- fixed axis system are defined by

$$A_{20} = \sqrt{\frac{3}{8}}\,\omega_Q[3\cos^2\beta - 1 + \eta\cos^2\beta\cos 2\alpha],$$

$$A_{2\pm1} = \frac{1}{2}\,\omega_Q \sin\beta\, e^{\mp i\gamma} \times [\pm(3 - \eta\cos 2\alpha)\cos\beta - i\eta\sin 2\alpha], \quad \text{and}$$

$$A_{2\pm2} = \frac{1}{2}\,\omega_Q e^{\mp 2i\gamma}\left[\frac{3}{2}\sin^2\beta + \frac{\eta}{2}(1 + \cos^2\beta)\cos 2\alpha \pm i\eta\cos\beta\sin 2\alpha\right]. \qquad [4]$$

The Euler angles (α, β, γ) describe the orientation of the principal axis system of the quadrupolar interaction in the rotor-fixed axis system, η denotes the asymmetry, and $\omega_Q = (e^2qQ/h)/[2S(2S - 1)]$ is the quadrupole frequency. The spherical spin tensor components are given by (*22–25, 31*)

$$T_{20} = \frac{1}{\sqrt{6}}[3S_z^2 - S(S+1)],$$

$$T_{2\pm1} = \mp\frac{1}{2}[S_\pm S_z + S_z S_\pm], \quad \text{and}$$

$$T_{2\pm2} = \frac{1}{2}(S_\pm)^2. \qquad [5]$$

As in the spin-$\frac{1}{2}$ case, the calculation of an effective Hamiltonian proceeds by transforming to an interaction representation. An analogous approach is used to describe the influence of chemical shielding interactions in the context of homonuclear dipolar recoupling (*38, 39*). We simplify the problem using the zeroth-order contribution in Eq. [2] to define the unitary operator

$$U(t) = \exp\left[-i\left[\int_0^t A_{20}(\tau)d\tau\right]T_{20}\right]. \qquad [6]$$

Following the notation of Vega (*20, 21*), the components of the RF interaction $S_x = 2C_x + T_x$ are given by

$$C_x = \frac{1}{2}\left(\left|\frac{1}{2}\right\rangle\left\langle\frac{-1}{2}\right| + \left|\frac{-1}{2}\right\rangle\left\langle\frac{1}{2}\right|\right), \quad \text{and}$$

$$T_x = \frac{\sqrt{3}}{2}\left(\left|\frac{3}{2}\right\rangle\left\langle\frac{1}{2}\right| + \left|\frac{1}{2}\right\rangle\left\langle\frac{3}{2}\right| + \left|\frac{-1}{2}\right\rangle\left\langle\frac{-3}{2}\right| + \left|\frac{-3}{2}\right\rangle\left\langle\frac{-1}{2}\right|\right). \qquad [7]$$

The transformation $\tilde{H}_Q = \exp(-i\zeta(t)T_{20})S_x\exp(i\zeta(t)T_{20})$ is easily performed using the eigenbasis of the single-transition operator $S_z(|\frac{3}{2}\rangle, \langle\frac{1}{2}|, |\frac{-1}{2}\rangle, \langle\frac{-3}{2}|)$. In this representation, the spin tensor component of the quadrupolar coupling can be expressed as

$$T_{20} = \frac{3}{\sqrt{6}}\left[\left(\left|\frac{3}{2}\right\rangle\left\langle\frac{3}{2}\right| + \left|\frac{-3}{2}\right\rangle\left\langle\frac{-3}{2}\right|\right) - \left(\left|\frac{1}{2}\right\rangle\left\langle\frac{1}{2}\right| + \left|\frac{-1}{2}\right\rangle\left\langle\frac{-1}{2}\right|\right)\right]. \quad [8]$$

Thus, only the triple-quantum coherence operator is altered by the transformation (Eq. [6]):

$$T_x \rightarrow e^{2i(3/\sqrt{6})\zeta(t)}\left(\left|\frac{3}{2}\right\rangle\left\langle\frac{1}{2}\right| + \left|\frac{-3}{2}\right\rangle\left\langle\frac{-1}{2}\right|\right)\frac{\sqrt{3}}{2} + e^{-2i(3/\sqrt{6})\zeta(t)}\left(\left|\frac{1}{2}\right\rangle\left\langle\frac{3}{2}\right| + \left|\frac{-1}{2}\right\rangle\left\langle\frac{-3}{2}\right|\right)\frac{\sqrt{3}}{2}. \quad [9]$$

Using

$$S_yS_z + S_zS_y = \frac{i\sqrt{3}}{2}\left(\left(\left|\frac{3}{2}\right\rangle\left\langle\frac{1}{2}\right| + \left|\frac{-3}{2}\right\rangle\left\langle\frac{-1}{2}\right|\right) - \left(\left|\frac{1}{2}\right\rangle\left\langle\frac{3}{2}\right| + \left|\frac{-1}{2}\right\rangle\left\langle\frac{-3}{2}\right|\right)\right), \quad [10]$$

we obtain

$$\tilde{H} = \omega_S(2C_x + \cos(\zeta(t))T_x + \sin(\zeta(t))(S_yS_z + S_zS_y)). \quad [11]$$

The time-dependent spatial components of the quadrupolar interaction are

$$\zeta(t) = \sqrt{6}\sum_{m'=-2}^{2}\frac{d_{0m'}(\Theta_M)A_{2m'}(\alpha, \beta, \gamma)}{im'\omega_r}(e^{im'\omega_r t} - 1). \quad [12]$$

Equation [11] can also be compared to the results for an $S = 1$ system (*41, 42*) in which the anticommutator of Eq. [11] represents antiphase single-quantum magnetization. In addition, identifying T_x with S_x and neglecting the central-transition operator lead us to the $S = 1$ result. In the spin-$\frac{3}{2}$ case, the coefficient for T_x in Eq. [11] describes a rotation between the central-transition and triple-quantum subspaces and is responsible for the adiabatic transfer of coherence between these two subspaces at a rate of multiples of the MAS frequency during spin locking. This rotation-induced adiabatic coherence transfer (RIACT) phenomenon (*7*) has been proposed for efficient excitation and reconversion of triple-quantum coherence. In Fig. 1a the behavior predicted by using the effective Hamiltonian of Eq. [11] is compared to the result of a numerical simulation (Fig. 1b) using Eq. [1], with $e^2qQ/h = 1.2$ MHz, an MAS frequency of 6 kHz, and a Larmor frequency of 105 MHz (i.e., ^{23}Na at 9.4 T). In both cases, the initial condition for testing adiabatic coherence transfer is $\rho(0) = C_x$, and polarization transfer is measured by the expectation value determined from the equation of motion

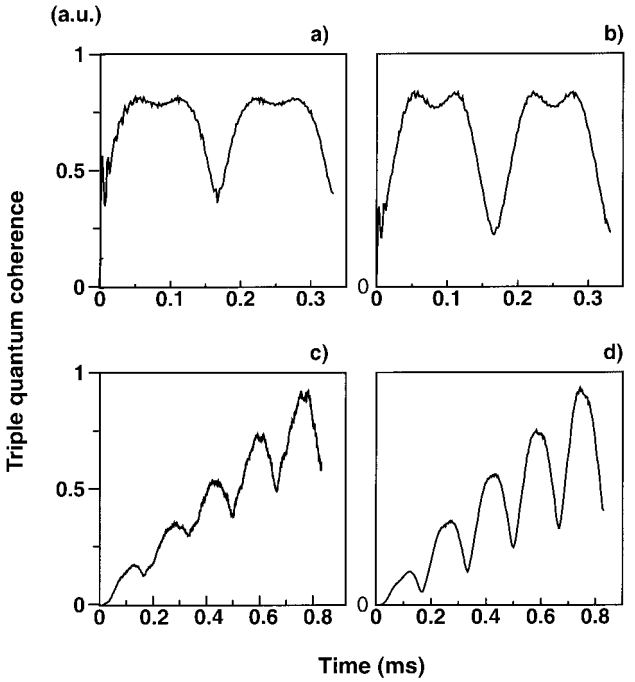

FIG. 1. (a, b) Comparison of (a) evolution of triple-quantum coherence using the effective Hamiltonian given in Eq. [11] and (b) the exact numerical prediction using the Hamiltonian of Eq. [1]. MAS spinning frequency and RF field strength were set to 6 and 50 kHz, respectively. The offset was chosen to compensate the first-order isotropic quadrupolar shift. The quadrupole coupling constant $e^2qQ/h = 1.2$ MHz was assumed. All numerical simulations were performed in the programming environment GAMMA (*50*). The initial condition in (a) and (b) is central-transition coherence, $\rho(0) = C_x$. (c, d) Comparison of triple-quantum coherence transfer (c) using the effective Hamiltonian of Eq. [15] and (d) using the exact Hamiltonian of Eq. [1], including the heteronuclear dipolar contribution as given in Eq. [15]. A heteronuclear dipolar coupling of 1.5 kHz was assumed. An RF field strength of 94 kHz was employed on the I spin. The initial condition for (c) and (d) is $\rho(0) = I_x$.

$$\langle A\rangle(t) = \mathrm{Tr}\{A\sigma(t)\}, \quad [13]$$

with $A = R_x$ and $\sigma(t) = U(t)C_xU^{-1}(t)$. Here, the triple-quantum coherence is defined by

$$R_x = \frac{1}{2}\left(\left|\frac{3}{2}\right\rangle\left\langle\frac{-3}{2}\right| + \left|\frac{-3}{2}\right\rangle\left\langle\frac{3}{2}\right|\right). \quad [14]$$

In Figs. 1a and 1b, an RF field of 50 kHz on the S spins was assumed. The MAS-modulated quadrupolar coupling acts as a recoupling element that connects the central and triple-quantum subspaces in a periodic manner. It should be noted that

Eqs. [11] and [12] predict that at multiples of a rotor period, $t = nT_r$, a nonvanishing amount of triple-quantum coherence remains since $\zeta(nT_r) = 0$. This effect has been experimentally observed previously (*7*). In addition, the dependence of the transfer rate $\zeta(t)$ upon the Euler angles (α, β, γ) determines the efficiency of the MQ exchange.

Due to the explicit definition of the spherical tensor operators, the total Hamiltonian of a dipolar-coupled ($I = \frac{1}{2}$, $S = \frac{3}{2}$) spin pair can easily be included in Eq. [11]. The dipolar contribution commutes with the zeroth-order quadrupolar interaction and we obtain

$$\tilde{H} = \omega_I I_x + D(t) I_z S_z + \omega_S (2C_x + \cos(\zeta(t)) T_x + \sin(\zeta(t))(S_y S_z + S_z S_y)). \quad [15]$$

$D(t)$ represents the MAS-modulated dipolar coupling and is given by

$$D_{\pm 1} = -\frac{D'}{2\sqrt{2}} \sin(2\beta_d) e^{\pm i\gamma_d},$$

$$D_{\pm 2} = \frac{D'}{4} \sin^2(\beta_d) e^{\pm 2i\gamma_d}, \quad \text{and}$$

$$D' = -\frac{\mu_0 \gamma_I \gamma_S h}{4\pi r^3}, \quad [16]$$

where β_d and γ_d are the polar angles that describe the direction of the internuclear dipolar vector $\vec{r}$ in a rotor-fixed coordinate system with its z axis along the sample rotation axis. γ_k represents the gyromagnetic ratio for spin I and S, respectively. Obviously, the spin operators are now given by the product base $|m, n\rangle$ with $m = \pm\frac{1}{2}$ and $n = \pm\frac{1}{2}, \pm\frac{3}{2}$.

Based on the results of Eqs. [11]–[15], we will now predict the CP dynamics for the cases of weak and strong RF fields applied to the S spins under simultaneous I spin irradiation (of strength ω_I).

Weak RF Fields

If we neglect the perturbation contribution in Eq. [15], we can elucidate the coherence transfer dynamics by transforming into a tilted frame $\tilde{H}^T = \exp[-i(\Theta_I I_y + \Theta_S C_y)]\tilde{H} \exp[+i(\Theta_I I_y + \Theta_S C_y)]$ with $\Theta_I = \Theta_S = \pi/2$. In this frame, the RF contributions are diagonal and time independent as in the usual spin-$\frac{1}{2}$ situation. The Hamiltonian commutes with the initial condition C_x and spin locking is possible. Application of Floquet (*16*) or average Hamiltonian theory (*43*) then gives the zero- and double-quantum matching conditions,

$$\omega_I \mp 2\omega_S = n\omega_r, \quad [17]$$

which result in the observable signal (central-transition coherence)

$$\langle C_x \rangle(t) = \pm\frac{1}{2} \int_0^\pi [1 - \cos(d_n(\theta_d)t)] \sin(\theta_d) d\theta_d, \quad [18]$$

with $\sigma(0) = I_x$. This behavior is analogous to transient oscillations observed both in the liquid (*44*) and in the solid state of spin-$\frac{1}{2}$ systems (*45*). Experimental results (data not shown) on a number of different ^{23}Na compounds confirm the validity of this concept for quadrupolar species. Also note that in this approximation, no triple-quantum coherence is generated. For these reasons, we will refer in the following to coherence transfer in the presence of small RF fields as single-quantum cross-polarization (SQCP) transfer. For increasing RF fields, the zero- and double-quantum conditions of Eq. [17] will be less well defined, and we expect a superposition of positive and negative transfer amplitudes to attenuate the transfer efficiency.

Strong RF Fields

We now turn to the case in which the time-dependent RIACT effect in Eqs. [11] and [15] cannot be neglected. As shown in the single spin $S = \frac{3}{2}$ case, this regime corresponds to the case of strong RF fields. Additional insight might be gained by introducing a new tilted coordinate system (defined by $(\pi/2)I_y + \Theta_S(t)C_y$, where C_y represents a transformation which renders the RF term diagonal). In this frame, the effective dipolar coupling will be further modulated by the time-dependent RF terms $\zeta(t)$, *leading to additional TQCP matching conditions (i.e., $I_x \rightarrow T_x$ transfer) that may deviate from the result of Eq. [17]*. Straightforward diagonalization of the Hamiltonian of Eq. [17], for example, shows that the eigenvalues are now explicitly dependent on $\zeta(t)$. These nonzero contributions will also lead to an explicit dependence of the matching conditions upon the single-crystallite orientation defined by the Euler angles given in Eqs. [4] and [16]. As in the extreme case of NQR (*46*), TQCP transfer will also occur for noninteger multiples of the spinning frequency around the $n = 0, \pm 1, \pm 2$ matching conditions. Likewise, the buildup of triple-quantum polarization will be governed by the combined modulation of RIACT quadrupolar transfer and the generally slower dipolar transfer $I \rightarrow S$. This behavior is illustrated in Figs. 1c and 1d, again comparing the numerical results using Eq. [1] (including the I-spin terms of Eq. [15]) to the theoretical predictions of Eq. [15]. In this case, an I, S dipolar coupling of 1.5 kHz was assumed and RF fields of $\omega_I = 94$ kHz and $\omega_S = 50$ kHz were employed. For a MAS frequency of 6 kHz, this condition corresponds to the $n = -1$ condition of Eq. [17]. With the initial condition $\rho(0) = I_x$, both Hamiltonians lead to similar transfer characteristics, with a monotonic signal growth modulated by the RIACT phenomenon. In analogy to the low RF field case outlined previously, we will in the following use the term triple-quantum cross polarization (TQCP) whenever the CP experiment is optimized for transfer steps involving

triple-quantum coherence. This behavior could be further described by a "second averaging" (*47*) approach in which a slow coherence transfer $I_x \rightarrow C_x$ (given by the dipolar coupling constant) at the SQ conditions of Eq. [17] is followed by a fast (MAS dictated) RIACT from single- to triple-quantum coherence to generate the TQCP signal. Alternatively, Floquet theory could be used after a Fourier analysis of the MAS-modulated RF field to elucidate the TQCP matching profile.

Additional simulations for a dipolar-coupled ^{1}H–^{17}O spin system indicate that the same mechanism outlined above also leads to the creation of 5-quantum coherence in an $I = \frac{1}{2}$, $S = \frac{5}{2}$ spin system. Using the same simulation environment, it is also possible to observe the excitation of triple-quantum coherence in a spin $I = \frac{1}{2}$, $S = \frac{5}{2}$ system such as recently reported by Ashbrook *et al.* (*48*). However, our numerical results do not agree with the experimental findings of Ashbrook *et al.* (*48*), which might be explained by a combined influence of nutation and spin-locking effects in a spin-$\frac{5}{2}$ system.

EXPERIMENTS AND DISCUSSION

To test the theoretical predictions of the previous section, we have employed the pulse sequence depicted in Fig. 2a, where 3Q coherence is immediately converted into observable central-transition coherence by a RIACT pulse. We have generally observed a superior reconversion efficiency of the RIACT pulse in comparison to nutation approaches (*7, 9, 18, 19, 42*). The phase of the spin-locking pulse on the *S* channel is cycled in 30° steps synchronously with phase cycling of the receiver by 90° steps to detect only 3Q coherence. Additionally, the sequence employs spin–temperature alternation (*42*) of the CP signal to suppress directly excited signals.

Experimental results on sodium acetate are shown in Fig. 3 for which we observe substantial triple-quantum polarization transfer in the range $\omega_{\mathrm{RF},^1\mathrm{H}} \in [80, 120]$ kHz. After a mixing time of 2 ms, the resulting triple-quantum signal was recorded as a function of proton RF field strength. For comparison, numerical simulations using quadrupolar, dipolar, and RF parameters as given in the figure caption are shown in Fig. 3. The quadrupolar parameters ($e^2qQ/h = 1.6$ MHz, $\eta = 0.7$) were obtained using a Floquet analysis (*22–25, 35, 49*) in the context of the GAMMA NMR simulation environment (*50*). The general trend is well reproduced, although with a smaller total matching range as shown in Fig. 3. This discrepancy can be at least partially attributed to RF inhomogeneity effects that are known to significantly broaden the matching profile in spin-$\frac{1}{2}$ applications (*45*). Moreover, multispin flips among nearby protons can further influence the experimental results (*43*).

In spin-$\frac{1}{2}$ Hartmann–Hahn CP experiments, considerable progress has recently been made to enhance the polarization transfer using adiabatic (*51*) transfer methods—e.g., by varying RF field amplitudes (*17, 45*) or the MAS frequencies (*52*). In the present case, this adiabatic variation of the dipolar-coupling Hamiltonian should not be confused with the "adiabatic passage" spin-locking regime defined by Vega (*20, 21*). Briefly, adiabatic polarization transfer is most efficiently achieved if the rate of amplitude change is smaller than the dipolar coupling and thus much smaller than the quadrupolar coupling that drives RIACT. We may therefore expect an additional gain in TQCP transfer efficiency if the amplitude variation is slow in comparison to these interactions and does not interfere with RIACT. This is most easily achieved by performing an amplitude variation on the *I* spins (Fig. 2b). In addition, the matching profile is characterized by a broad distribution of matching conditions for which we may expect an increased overall transfer efficiency. To discriminate between both effects, additional experiments that reverse the adiabatic transfer (*17, 45*) could be employed. In the present context, it is sufficient to study the resulting signal enhancement that is experimentally illustrated in Fig. 4. In agreement with numerical simulations, we observed a signal enhancement of more than 50%. In the case of sodium acetate, an optimum amplitude sweep of 8% about the square pulse power at maximum transfer (corresponding to a change in RF field of ±3 kHz) was observed.

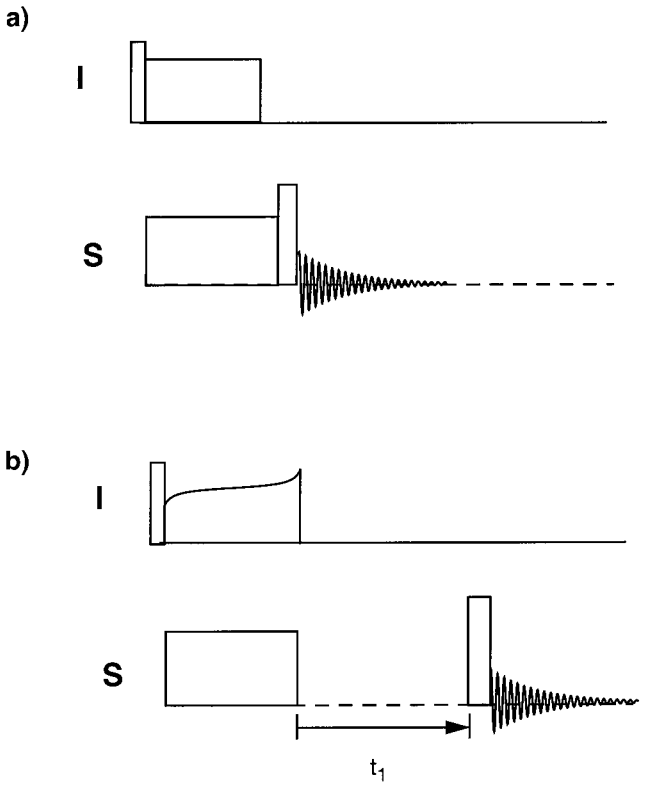

FIG. 2. (a) Experimental pulse scheme to observe triple-quantum cross polarization (TQCP). After an initial 90° pulse on the *I* spins (in our case ^{1}H), polarization transfer occurs during a subsequent mixing time (typically 1–10 ms). Triple-quantum coherence is subsequently reconverted by a RIACT (*7*) pulse. (b) Optimized TQCP experiment in the context of a high-resolution MQMAS (*2, 3*) experiment. An adiabatic modulation of TQCP is introduced on the spin-$\frac{1}{2}$ (*I* spin) channel and a triple-quantum evolution time after TQCP mixing is used prior to reconversion and detection.

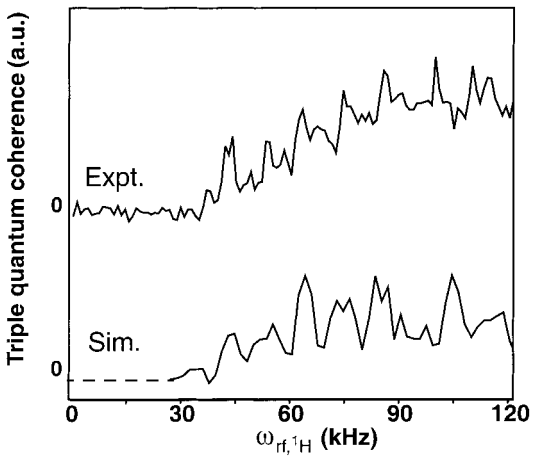

FIG. 3. Comparison between experimental and numerically predicted TQ matching as observed in sodium acetate for a contact time of 2 ms and variable ^{1}H RF field strength. For the numerical simulation, an isolated two-spin ($I = \frac{1}{2}$, $S = \frac{3}{2}$) system was assumed using RF fields of 94 and 50 kHz on I and S spins, respectively. As in Fig. 1, a dipolar coupling of 1.5 kHz was used and the initial density matrix was $\rho(0) = I_x$.

Of particular interest is the relative sensitivity of the TQCP method with respect to SQCP during MQMAS experiments. In general, the TQCP method eliminates the excitation (or reconversion) step connecting central and triple-quantum coherence. A comparison can be attempted by accurately optimizing the SQCP and TQCP matching conditions and comparing the following transfer steps:

$$I_x \xrightarrow{\text{SQCP}} C_x \xrightarrow{\text{nutation}} T_x \xrightarrow{\text{RIACT}} C_x, \quad \text{and}$$

$$I_x \xrightarrow{\text{TQCP}} T_x \xrightarrow{\text{RIACT}} C_x.$$

However, one should keep in mind that additional experimental parameters can seriously influence this comparison. For the SQCP method the polarization transfer efficiency is influenced by offset terms and the superposition of zero- and double-quantum terms (see Eq. [17]). In general, careful adjustment and stability of the RF power level are required to ensure efficient transfer. In addition, an increased RF bandwidth for SQCP (such as in the presence of significant chemical shift terms) will result in a reduced efficiency for the transfer. Both effects are less problematic for the TQCP approach, for which high RF fields can be employed over a wide range of RF power levels. Experimentally, we have observed TQCP transfer efficiencies for sodium acetate that were at least a factor 2 higher than for the SQCP approach. On the other hand, simulations indicate that the SQCP approach is superior in the presence of small dipolar couplings. These numerical predictions were experimentally observed on anhydrous Na_2HPO_4, in which the dipolar ^{1}H–^{23}Na couplings are known to be smaller (*53*). While in the context of dipolar filtering this behavior can further simplify the spectral analysis, we are currently also investigating experimental modifications that enhance the TQCP efficiency for larger distances.

To illustrate the filtering that can be achieved with TQCP, we performed ^{23}Na experiments on a test sample consisting of sodium acetate and aprotic sodium sulfate. The left column of Fig. 5 shows a standard one-pulse decay spectrum under MAS and a TQCP-filtered MAS spectrum. A superposition of two lineshapes is expected in the one-pulse MAS spectrum corresponding to the residual second-order quadrupolar broadening under MAS. In the TQCP-filtered spectrum, no signal due to sodium sulfate is observed. In the right-hand column of Fig. 5 we show two MQMAS spectra (using the t_1 evolution in Fig. 2b) which demonstrate the utility of the TQCP filter. Only the isotropic signal from sodium acetate is retained in the TQCP-MAS experiment.

In spin-$\frac{1}{2}$ cases, the polarization transfer characteristics of an isolated spin-$\frac{1}{2}$ pair are symmetric; i.e., the efficiency of the transfer is not influenced by the initial condition (nonzero polarization on I or S spin). Our theoretical and numerical results indicate that this behavior also applies to the multiple-quantum transfer methods discussed in this contribution. It is thus also possible to directly transfer triple-quantum coherence from a quadrupolar nucleus to the spin-$\frac{1}{2}$ nucleus with equal efficiency. Starting with a conventional MQMAS experiment, in which multiple-quantum coherence is evolved for time t_1 on the quadrupolar nucleus, a subsequent TQCP transfer to the

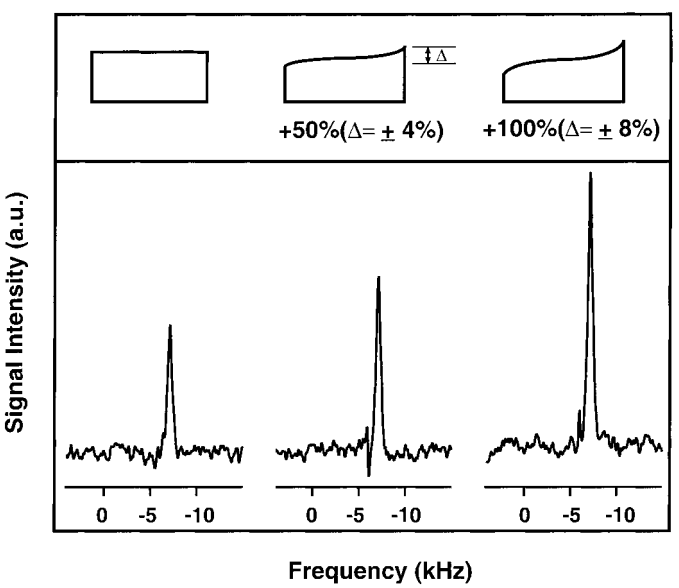

FIG. 4. Comparison of experimentally observed signal enhancements in sodium acetate resulting from a tangential modulation of the I spin RF field strength. Radiofrequency modulations (as indicated by Δ) are centered on the maximum TQCP matching condition determined experimentally in Fig. 3.

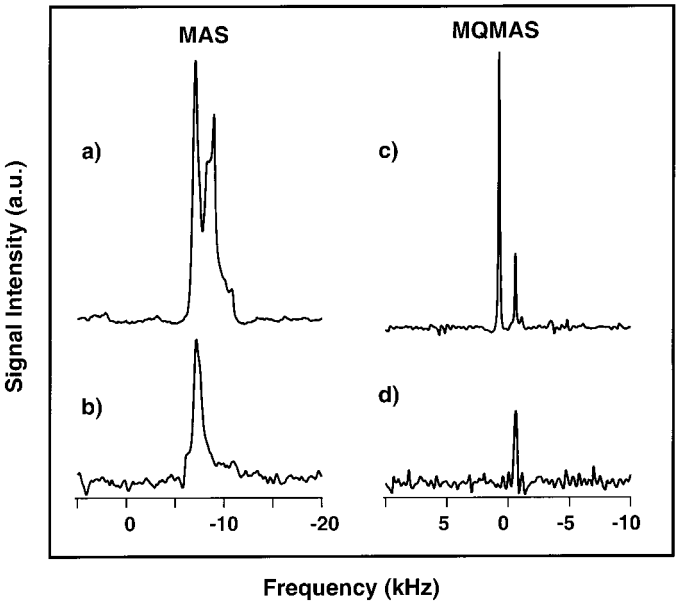

FIG. 5. Experimental results on a sodium acetate/sodium sulfate mixture. In the left column, conventional single-pulse spectra (upper trace) are compared to a TQCP-filtered spectrum. MQMAS spectra (right column) are shown without (upper trace) and with TQCP filtering (see Fig. 2b).

spin-$\frac{1}{2}$ coupling partner followed by t_2 detection would provide a high-resolution, 2D heteronuclear correlation spectrum. This modification of the experimental techniques outlined in Fig. 2 would also be advantageous whenever the spin-$\frac{1}{2}$ spin–lattice relaxation time is significantly longer than the quadrupolar T_1 relaxation time.

CONCLUSIONS

Heteronuclear polarization transfer represents one of the key elements for structure elucidation in spin-$\frac{1}{2}$ applications. In these cases, the cross-polarization dynamics in an isolated two-spin pair are well understood.

In this contribution we have investigated extensions of this approach to heteronuclear spin systems involving quadrupolar nuclei. In the quadrupolar case, a more detailed analysis of the influence of RF and dipolar interactions under MAS is needed. We have shown that an effective Hamiltonian can be derived to describe the central-transition spin-locking behavior of a quadrupolar nucleus. In the same formalism, the RIACT concept to excite and reconvert multiple-quantum coherence can be understood as a MAS-induced rotation between central and triple-quantum transition subspaces of an $S = \frac{3}{2}$ spin system. In the context of high-resolution MQMAS applications, it is possible to directly transfer spin-$\frac{1}{2}$ polarization into multiple-quantum polarization. The effective Hamiltonian derived for an isolated quadrupolar spin under MAS also provides analytical insight into the dynamics of an I, S spin system subjected to RF fields and MAS. In particular, we have shown that by employing medium-size (i.e., in the order of 50 kHz) RF fields on the quadrupolar nucleus, it is possible to directly cross polarize into the triple-quantum coherence. Thus, TQCP transfer can act as a dipolar filter for the subsequent high-resolution (MQMAS) part of the experiment. This scheme can also be adapted for a 2D HETCOR experiment (displaying high resolution in two dimensions), by introducing an additional evolution time after the preparatory $\pi/2$ pulse on the spin-$\frac{1}{2}$ nuclei. Comparative studies between a conventional single-quantum (SQ) CP experiment and the TQCP method indicate that the latter approach leads to a 2–5 times higher overall transfer efficiency for large- or medium-size dipolar couplings. For small dipolar couplings (below 500 Hz), this gain cannot be realized and we are planning further investigations to optimize the transfer also for longer distances. Preliminary results indicate that adiabatic TQCP techniques can substantially improve the transfer efficiency. Here, adiabaticity refers to a slow variation of the RF field amplitude on the spin-$\frac{1}{2}$ nucleus during TQCP mixing.

The outlined concept of direct creation of multiquantum coherence during the CP process might also be employed in the context of generating double-quantum coherence among strongly dipolar-coupled spin-$\frac{1}{2}$ nuclei such as ^{13}C–^{1}H or ^{1}H–^{1}H systems.

ACKNOWLEDGMENTS

We thank Mr. C. M. Rienstra and Dr. J. D. Gross for making the MAS probes available to us. Early collaborations and discussions with Prof. Gang Wu are gratefully acknowledged. M.B. gratefully acknowledges financial support by a DFG research fellowship. This work was supported by Grants GM-23403 and RR-00995.

REFERENCES

1. S. J. Lippard and J. M. Berg, "Principles of Bioinorganic Chemistry," University Science Books, Mill Valley, CA (1994).
2. L. Frydman and J. S. Harwood, *J. Am. Chem. Soc.* **117,** 5367 (1995).
3. A. Medek, J. S. Harwood, and L. Frydman, *J. Am. Chem. Soc.* **117,** 12779–12787 (1995).
4. G. Wu, D. Rovnyak, B. Sun, and R. G. Griffin, *Chem. Phys. Lett.* **249,** 210–217 (1996).
5. C. Fernandez and J.-P. Amoureux, *Chem. Phys. Lett.* **242,** 449–454 (1995).
6. G. Wu, D. Rovnyak, P. C. Huang, and R. G. Griffin, *Chem. Phys. Lett.* **277,** 79–83 (1997).
7. G. Wu, D. Rovnyak, and R. G. Griffin, *J. Am. Chem. Soc.* **118,** 9326–9332 (1996).
8. D. Massiot, *J. Magn. Reson. A* **122,** 240–244 (1996).
9. J.-P. Amoureux, C. Fernandez, and L. Frydman, *Chem. Phys. Lett.* **259,** 347–355 (1996).
10. U.-T. Pingel, J.-P. Amoureux, T. Anupold, F. Bauer, H. Ernst, C. Fernandez, D. Freude, and A. Samosan, *Chem. Phys. Lett.* **294,** 345–350 (1998).
11. C. Fernandez and J.-P. Amoureux, *Solid State Nucl. Magn. Reson.* **5,** 315–321 (1996).

12. S. R. Hartmann and E. L. Hahn, *Phys. Rev.* **128,** 2042–2053 (1962).
13. A. Pines, M. G. Gibby, and J. S. Waugh, *J. Chem. Phys.* **59,** 569–590 (1973).
14. M. Levitt, D. Suter, and R. R. Ernst, *J. Chem. Phys.* **84,** 4243–4255 (1986).
15. A. Verhoeven, R. Verel, and B. H. Meier, *Chem. Phys. Lett.* **266,** 465–472 (1997).
16. S. Hediger, B. H. Meier, and R. R. Ernst, *J. Chem. Phys.* **102,** 4000–4011 (1995).
17. M. Baldus, D. G. Geurts, S. Hediger, and B. H. Meier, *J. Magn. Reson. A* **118,** 140 (1996).
18. S. Vega, *Phys. Rev. A* **23,** 3152–3173 (1981).
19. S. Vega and Y. Naor, *J. Chem. Phys.* **75,** 75–86 (1981).
20. A. J. Vega, *Solid State Nucl. Magn. Reson.* **1,** 17–32 (1992).
21. A. J. Vega, *J. Magn. Reson.* **96,** 50–68 (1992).
22. D. Freude and J. Haase, "Quadrupole Effects in Solid-State Magnetic Resonance," NMR Basic Principles and Progress, Vol. 29, Springer Verlag, Berlin (1993).
23. C. P. Slichter, "Principles of Magnetic Resonance," Springer-Verlag, Berlin (1978).
24. B. F. Chmelka and J. W. Zwanziger, "Quadrupole Effects in Solid-State Magnetic Resonance," NMR Basic Principles and Progress, Vol. 33, Springer-Verlag, Berlin (1994).
25. A. P. M. Kentgens, *Geoderma* **80,** 271 (1997).
26. C. A. Fyfe, H. Grondey, K. T. Mueller, K. C. Wong-Moon, and T. Markus, *J. Am. Chem. Soc.* **114,** 5876–5878 (1992).
27. C. S. Blackwell and R. L. Patton, *J. Phys. Chem.* **88,** 6135–6139 (1984).
28. R. K. Harris and G. J. Nesbitt, *J. Magn. Reson.* **78,** 245–256 (1988).
29. C. Fernandez, L. Delevoye, J.-P. Amoureux, D. P. Lang, and M. Pruski, *J. Am. Chem. Soc.* **119,** 6858–6862 (1997).
30. S. H. Wang, S. M. De Paul, and L. M. Bull, *J. Magn. Reson.* **125,** 364–368 (1997).
31. M. Mehring, "Principles of High Resolution NMR in Solids," Springer-Verlag, Berlin (1983).
32. U. Haeberlen, "High Resolution NMR Spectroscopy in Solids," Academic Press, San Diego (1976).
33. J. H. Shirley, *Phys. Rev. B* **4,** 979–987 (1965).
34. A. Schmidt and S. Vega, *J. Chem. Phys.* **87,** 6895–6907 (1987).
35. T. O. Levante, M. Baldus, B. H. Meier, and R. R. Ernst, *Mol. Phys.* **86,** 1195 (1995).
36. M. Baldus, D. Rovnyak, and R. G. Griffin, MAS assisted multiquantum recoupling in quadrupolar spin systems, #MT101, *in* "40th Experimental Nuclear Magnetic Resonance Conference," Orlando, FL, 1999.
37. J. J. Sakurai, "Modern Quantum Mechanics," Addison-Wesley, Reading, MA (1994).
38. M. H. Levitt, D. P. Raleigh, F. Creuzet, and R. G. Griffin, *J. Chem. Phys.* **92,** 6347–6364 (1990).
39. M. G. Colombo, B. H. Meier, and R. R. Ernst, *Chem. Phys. Lett.* **146,** 189–196 (1988).
40. M. M. Maricq and J. S. Waugh, *J. Chem. Phys.* **70,** 3300 (1979).
41. O. W. Sorensen, G. W. Eich, M. H. Levitt, G. Bodenhausen, and R. R. Ernst, *Prog. NMR Spectrosc.* **16,** 163 (1983).
42. R. R. Ernst, G. Bodenhausen, and A. Wokaun, "Principles of Nuclear Magnetic Resonance in One and Two Dimensions," Clarendon, Oxford (1987).
43. E. O. Stejskal, J. Schaefer, and J. S. Waugh, *J. Magn. Reson.* **28,** 105–112 (1977).
44. L. Mueller, A. Kumar, T. Baumann, and R. R. Ernst, *Phys. Rev. Lett.* **32,** 1402–1406 (1974).
45. S. Hediger, "Improvement of Heteronuclear Polarization Transfer in Solid-State NMR," Ph.D., thesis, ETH, Zurich, 1997.
46. R. Tycko, *Phys. Rev. Lett.* **58,** 2281–2284 (1988).
47. M. Goldman, P. J. Grandinetti, A. Llor, Z. Olejiniczak, J. R. Sachleben, and J. W. Zwanziger, *J. Chem. Phys.* **97,** 8947 (1992).
48. S. Ashbrook, S. Brown, and S. Wimperis, *Chem. Phys. Lett.* **288,** 509 (1998).
49. M. Baldus, T. Levante, and B. H. Meier, *Zeit. Natur. A* **49,** 80 (1994).
50. S. A. Smith, T. O. Levante, B. H. Meier, and R. R. Ernst, *J. Magn. Reson. A* **106,** 75 (1994).
51. A. Abragam, "Principles of Nuclear Magnetism," Oxford Univ. Press, Oxford (1961).
52. R. Verel, M. Baldus, M. Nijman, J. W. M. van Os, and B. H. Meier, *Chem. Phys. Lett.* **280,** 31 (1997).
53. M. Baldus, B. H. Meier, R. R. Ernst, A. P. M. Kentgens, and H. Meyer zu Altenschildesche, *J. Am. Chem. Soc.* **117,** 5141 (1995).